

# Electromagnetic prompt response in an elastic wave cavity

A. M. Martínez-Argüello,<sup>1</sup> M. Martínez-Mares,<sup>1</sup> M. Cobián-Suárez,<sup>2</sup> G. Báez,<sup>2</sup> and R. A. Méndez-Sánchez<sup>3</sup>

<sup>1</sup>*Departamento de Física, Universidad Autónoma Metropolitana-Iztapalapa,  
Apartado Postal 55-534, 09340 México Distrito Federal, Mexico*

<sup>2</sup>*Departamento de Ciencias Básicas, Universidad Autónoma Metropolitana-Azcapotzalco,  
Apartado Postal 21-267, 04000 México Distrito Federal, Mexico*

<sup>3</sup>*Instituto de Ciencias Físicas, Universidad Nacional Autónoma de México,  
Apartado Postal 48-3, 62210 Cuernavaca Mor., Mexico*

A rapid, or prompt response, of an electromagnetic nature, is found in an elastic wave scattering experiment. The experiment is performed with torsional elastic waves in a quasi-one-dimensional cavity with one port, formed by a notch grooved at a certain distance from the free end of a beam. The stationary patterns are diminished using a passive vibration isolation system at the other end of the beam. The measurement of the resonances is performed with non-contact electromagnetic-acoustic transducers outside the cavity. In the Argand plane, each resonance describes a circle over a base impedance curve which comes from the electromagnetic components of the equipment. A model, based on a variation of Poisson's kernel is developed. Excellent agreement between theory and experiment is obtained.

PACS numbers: 46.40.Cd, 62.30.+d, 03.65.Nk, 73.21.Fg

The study of wave transport through cavities, or scattering properties in a more general sense, has received intense theoretical and experimental attention in recent years. On the one hand, special interest has been the fingerprint of the classical dynamics in wave systems [1–4], like lithographic quantum dots [5–8], microwave cavities [9–14] and graphs [15, 16]. On the other hand, most of the experiments on elastic systems with different geometries are mainly concerned with the analysis of the spectrum [17–21] or carried out in the time domain [22, 23]. Single-frequency scattering experiments on elastic systems are difficult to perform due to the formation of stationary patterns [24]. Also, the excitation and selection of a particular type of elastic motion is a difficult task with commercial piezoelectric transducers.

Recently, this has started to change due to the successful reduction of the stationary waves using absorbing materials [21, 25]. In addition, particular kinds of vibrations can be selectively excited or detected with different configurations of electromagnetic-acoustic transducers (EMATs) [19, 20, 26]. Although the use of EMATs provide the advantage of not being in contact with the system, the electromagnetic field of the exciter enters into the detector [25]. Therefore, the elastic scattering system as a whole, including the EMATs, presents an electromagnetic impedance which cannot be ignored. The resonances of the system lie on a base electromagnetic impedance curve that induces direct processes coming from an electromagnetic prompt response in the scattering of elastic waves, as well as the expected prompt response in the elastic waves. As will be shown below, the effect of this impedance can be taken into account in

the total prompt response of the system.<sup>1</sup>

In this Letter we present measurements of the  $1 \times 1$  scattering matrix, in a single port quasi-one-dimensional cavity, for torsional waves in a beam. In the Argand plane, the experimental scattering matrix moves along the impedance curve describing circles on each resonance of the cavity, as frequency is varied. That is, the measured scattering matrix consists of the scattering matrix of the cavity plus its displacement along that impedance curve. Here, the experimental results are described by taking into account this phenomenon in a theoretical model based on Poisson's kernel, an opposite to that in which the direct processes are subtracted in microwave measurements in cavities [27] and graphs [15].

The cavity is formed on a square-cross-section aluminum beam, as shown in Fig. 1, between a free end and a notch of width  $a$  and depth  $h$ , grooved at a distance  $L$  from the free end. At the other end of the beam a passive vibration isolation system is used. Torsional vibrations are induced using electromagnetic-acoustic transducers (EMATs). The signal of a vector network analyzer (VNA, Anritsu MS-4630B) is sent to a high-fidelity audio amplifier (Cerwin-Vega CV-900) and then to the EMAT exciter located at a certain distance from the notch, outside the cavity. The torsional acceleration is measured by another EMAT, just outside the cavity, and sent to the VNA. In this way the non-normalized  $1 \times 1$  scattering matrix,

$$S(f) = \sqrt{R(f)} e^{i\theta(f)}, \quad (1)$$

---

<sup>1</sup> Notice that this effect is not the same as that of Ref. [27] where direct reflections are induced by imperfect coupling to the system.

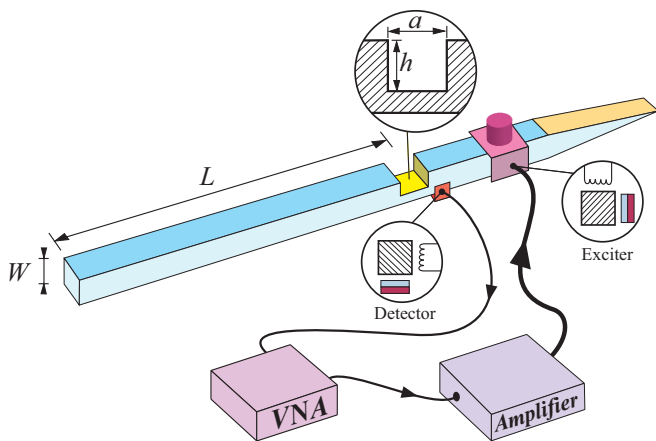


FIG. 1. Experimental setup used to form an open elastic wave system (not to scale). A cavity is formed in a beam by machining a notch in it at a certain distance from the free end. The total length of the beam is 3.6 m with a square cross-section of side  $W = 25.4$  mm;  $L = 2.5$  m,  $h = 18.0$  mm, and  $a = 0.9$  mm. The wedge is 40.0 cm long. The beam is supported by two nylon threads (not shown). The connection of the equipment is shown at the bottom. The exciter is located at 70 cm from the notch. Aluminum alloy 6061-T6, with shear modulus  $G = 26$  GPa and density  $\rho = 2.7$  g/cm<sup>3</sup>, was used.

where  $R(f)$  is the reflection coefficient and  $\theta(f)$  the phase, is measured for torsional waves.

A typical measurement is shown in Fig. 2, in which the magnitude and phase of  $S$  are plotted as a function of the frequency  $f$ , from 14000 to 20500 Hz. According to a simple theoretical model [25], eleven torsional resonances can be identified in this range of frequencies; they are indicated with vertical marks in the same figure. The remaining peaks correspond to other modes of vibration or to radio broadcasting stations [25]. It is noticeable that all resonances are located on a base line which comes from the electromagnetic impedance of the system as a whole (see also Fig. 3). This was verified by the null hypothesis that corresponds to the measurement without the elastic wave system.

In Fig. 3 the motion of  $S(f)$  in the complex plane is shown as a function of the frequency  $f$ . Instead of calibrating the scattering matrix as in Refs. [15, 27], an unnormalized  $S$ -matrix will be used and the experimental data will be given in arbitrary units. As expected,  $S(f)$  describes a circle for each resonance, but their centers are not located at the origin. In fact, the circles are superimposed on a base curve which is parallel to that obtained from the null hypothesis. The circles are not closed because the electromagnetic impedance is not constant but it varies slowly with frequency. Due to this fact each resonance is analyzed separately. In Fig. 3 the result of the null hypothesis is also shown in the Argand plane as the frequency is varied.

As has been recently shown by the authors [25, 28],

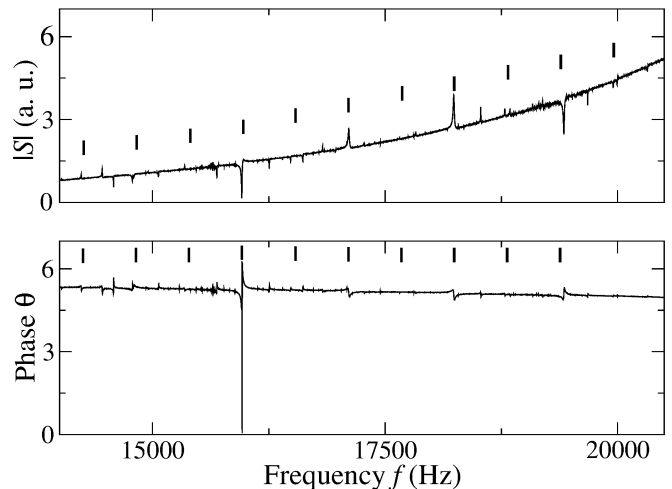


FIG. 2. The magnitude and phase of  $S(f)$ , showing the resonance spectrum measured with the detector located just outside the cavity. The vertical marks correspond to theoretical predictions [25].

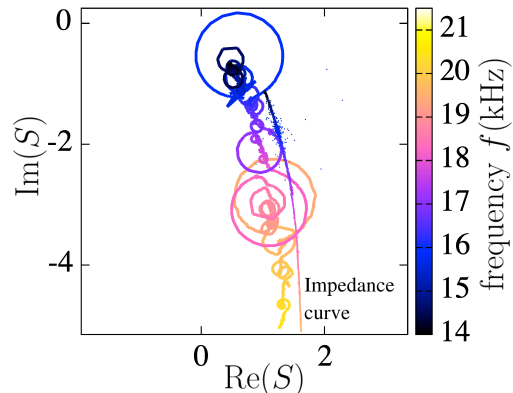


FIG. 3. (Color online) Motion of  $S(f)$  in the Argand plane as a function of frequency  $f$  for the same resonances of Fig. 2. The impedance curve, measured without the elastic system, is given by the thick line.

the scattering matrix of each resonance, as seen from the center of its own circle,  $S'(f)$ , visits the circumference in a non-uniform way, *i.e.*, according to Poisson's kernel

$$P'(S') = \frac{1}{2\pi} \frac{R' - |\overline{S'}|^2}{|S' - \overline{S'}|^2} \delta(R' - R_0), \quad (2)$$

where

$$S'(f) = \sqrt{R'} e^{i\theta'(f)}, \quad R' = R_0, \quad (3)$$

and  $R_0$  is a constant, experimentally determined as the square of the average of  $|S'(f)|$ . Here,  $\overline{S'} \equiv \overline{S'(f)}$  is the frequency average of  $S'(f)$ , also determined experimentally. In the jargon of nuclear physics this corresponds to the well known *optical scattering matrix* which accounts

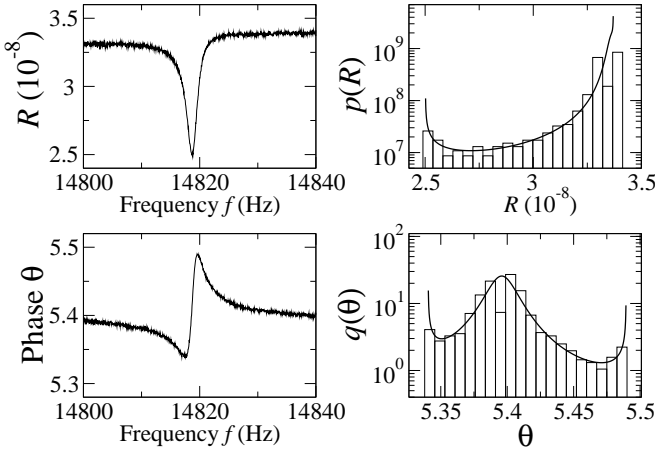


FIG. 4. Resonance at 14819 Hz. In the left panels the magnitude squared and phase of  $S(f)$  are shown. The histograms of the experimental data are compared with the theoretical expressions (continuous lines) of Eqs. (7) and (9).

for the prompt response of the system during the scattering processes. For the theoretical description of the experimental data, as originally measured, the effect of the electromagnetic impedance has to be taken into account.

From the known distribution of  $S'(f)$ , Eq. (2), the probability distribution of  $S(f)$  for each resonance can be obtained. Both scattering matrices are related by a translation,

$$S(f) = S'(f) + Z, \quad (4)$$

where  $Z$  is the position of the center of the circle, as seen from the origin; this displacement is triggered by the impedance, which is different for each resonance. This implies that the optical  $S$  matrix,  $S_{\text{opt}} \equiv \overline{S(f)}$ , consists of two parts: one coming from the scattering process of the system itself and a second coming from the electromagnetic components;

$$S_{\text{opt}} = \overline{S'} + Z. \quad (5)$$

From Eq. (2), the probability density distribution of  $S(f)$  is given by

$$P(S) = \frac{1}{2\pi} \frac{|S - Z|^2 - |S_{\text{opt}} - Z|^2}{|S - S_{\text{opt}}|^2} \delta[R'(S) - R_0], \quad (6)$$

where  $R'(S) = |S - Z|^2$ . In contrast to the ideal case where the impedance is absent and only  $S_{\text{opt}}$  is enough to describe the scattering in the system [29, 30], this distribution depends on two experimental parameters,  $S_{\text{opt}}$  and  $Z$ .  $R_0$  is a constant, not a parameter, whose value deviates from 1 due to the arbitrary units used in the measurements.

To visualize the distribution of  $S$ , the marginal distributions for  $R$  and  $\theta$  will be determined. To obtain the

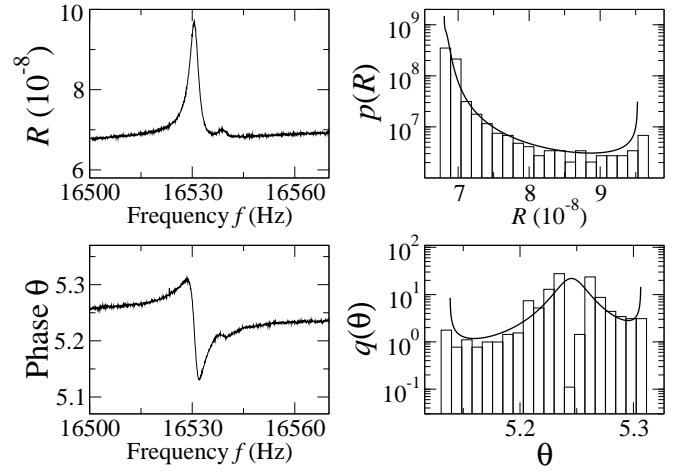


FIG. 5. Resonance at 16530 Hz. Excellent agreement is found between theory and experiment despite the appearance of a second type of resonance, not completely eliminated by the absorber.

distribution of  $R$ , Eq. (2) is integrated with respect to  $\theta$ . It is clear that the minimum and a maximum values of  $\sqrt{R}$  are imposed by  $Z$ ; that is, the minimum (maximum) is given by the sum of the distance to center  $|Z|$ , minus (plus) the radius of the circle  $\sqrt{R_0}$ . From Eq. (6) we obtain

$$p(R) = \frac{1}{2\pi} \frac{R_0 - |S_{\text{opt}} - Z|^2}{\sqrt{[R - (|Z| - \sqrt{R_0})^2][(|Z| + \sqrt{R_0})^2 - R]}} \times \left( \frac{1}{|\sqrt{R} e^{i\theta_+} - S_{\text{opt}}|^2} + \frac{1}{|\sqrt{R} e^{i\theta_-} - S_{\text{opt}}|^2} \right) \times [\Theta(|Z| + \sqrt{R_0} - \sqrt{R}) + \Theta(\sqrt{R} - |Z| + \sqrt{R_0})], \quad (7)$$

where  $\Theta(z)$  is the Heaviside function of  $z$  and

$$\sqrt{R} e^{i\theta_{\pm}} = \frac{1}{2Z^*} \left\{ (R + |Z|^2 - R_0) \pm i \sqrt{[R - (|Z| - \sqrt{R_0})^2][(|Z| + \sqrt{R_0})^2 - R]} \right\}. \quad (8)$$

In a similar way, the marginal phase distribution  $q(\theta)$  is obtained by integrating over  $R$ ; the result is

$$q(\theta) = \frac{1}{2\pi} \frac{R_0 - |S_{\text{opt}} - Z|^2}{\sqrt{R_0 - [\text{Im}(Z^* e^{i\theta})]^2}} \times \left( \frac{\sqrt{R_+}}{|\sqrt{R_+} e^{i\theta} - S_{\text{opt}}|^2} + \frac{\sqrt{R_-}}{|\sqrt{R_-} e^{i\theta} - S_{\text{opt}}|^2} \right) \times \left[ \Theta\left(\phi - \sin^{-1} \frac{\sqrt{R_0}}{|Z|} - \theta\right) + \Theta\left(\theta - \phi - \sin^{-1} \frac{\sqrt{R_0}}{|Z|}\right) \right], \quad (9)$$

where  $\phi$  is defined through  $e^{i\phi} = Z/|Z|$ ;

$$\sqrt{R_{\pm}} = \text{Re}(Z^* e^{i\theta}) \pm \sqrt{R_0 - [\text{Im}(Z^* e^{i\theta})]^2}, \quad (10)$$

and  $\text{Re}(z)$  and  $\text{Im}(z)$  stand for the real and imaginary parts of  $z$ .

In Figs. 4 and 5 the results for two typical experimental resonances, at 14819 and 16530 Hz, are shown. The left panels of both figures show the magnitude squared ( $R$ ) and phase ( $\theta$ ) of the amplitude of the measured signal; the effect of the impedance is noticeable. In the right panels the distributions for  $R$  and  $\theta$  are shown as histograms along with the theoretical expressions (continuous lines) for the marginal distributions, Eqs. (7) and (9). The only relevant parameters,  $S_{\text{opt}}$  and  $Z$ , were obtained from the experimental data. Despite the hollow that appears in the histograms of the phase, an excellent agreement is observed. The hollow is due to the lack of data since the experimental resonances does not close completely. In Fig. 5 one can observe that another resonance appears around 16540 Hz. The effect of this resonance, that belongs to another type of vibration not completely eliminated by the passive vibration isolation system, does not noticeably affect the distributions.

In conclusion, wave transport through a quasi-one-dimensional elastic cavity was studied. This was done by measuring the scattering matrix for torsional waves. The system was opened at one end by a passive vibration isolation system reducing substantially the presence of stationary waves. Although the excitation (and detection) of the modes was performed by non-contact electromagnetic-acoustic transducers, the exciter induces an electromagnetic impedance in the detector that affects dramatically the measurements. This effect was included in the theoretical description of the experiment as direct processes by adding a constant to the scattering matrix. The only relevant parameters, whose values were taken from the experiment, are the displacement due to the electromagnetic impedance and the optical scattering matrix of the elastic waves. An excellent agreement between the theoretical predictions and the experimental results was obtained.

This work was supported by DGAPA-UNAM under project PAPIIT IN103115. MCS and AMMA thank the financial support provided by CONACyT. MMM is grateful to the Sistema Nacional de Investigadores and MA Torres-Segura for her encouragement.

---

[1] P. A. Mello and N. Kumar, *Quantum Transport in Mesoscopic Systems: Complexity and Statistical Fluctuations* (Oxford University Press, New York, 2005).  
 [2] P. A. Mello, H. Baranger, AIP Conf. Proc. No. 464 (AIP, Melville, NY, 1999), p. 281.  
 [3] C. W. J. Beenakker, Rev. Mod. Phys. **69**, 731 (1997).  
 [4] Y. Alhassid, Rev. Mod. Phys. **72**, 895 (2000).

[5] C. M. Marcus, A. J. Rimberg, R. M. Westervelt, P. F. Hopkins, and A. C. Gossard, Phys. Rev. Lett. **69**, 506 (1992).  
 [6] A. M. Chang, H. U. Baranger, L. N. Pfeiffer, and K. W. West, Phys. Rev. Lett. **73**, 2111 (1994).  
 [7] I. H. Chan, R. M. Clarke, C. M. Marcus, K. Campman, and A. C. Gossard, Phys. Rev. Lett. **74**, 3876 (1995).  
 [8] M. W. Keller, A. Mittal, J. W. Sleight, R. G. Wheeler, D. E. Prober, R. N. Sacks, and H. Shtrikmann, Phys. Rev. B **53**, R1693 (1996).  
 [9] E. Doron, U. Smilansky, and A. Frenkel, Phys. Rev. Lett. **65**, 3072 (1990).  
 [10] H.-D. Gräf, H. L. Harney, H. Lengeler, C. H. Lewenkopf, C. Rangacharyulu, A. Richter, P. Schardt, and H. A. Weidenmüller, Phys. Rev. Lett. **69**, 1296 (1992).  
 [11] R. A. Méndez-Sánchez, U. Kuhl, M. Barth, C. H. Lewenkopf, and H.-J. Stöckmann, Phys. Rev. Lett. **91**, 174102 (2003).  
 [12] U. Kuhl, M. Martínez-Mares, R. A. Méndez-Sánchez, and H.-J. Stöckmann, Phys. Rev. Lett. **94**, 144101 (2005).  
 [13] H. Schanze, H.-J. Stöckmann, M. Martínez-Mares, and C. H. Lewenkopf Phys. Rev. E **71**, 016223 (2005).  
 [14] J. A. Franco-Villafañe, E. Sadurní, S. Barkhofen, U. Kuhl, F. Mortessagne, and T. H. Seligman, Phys. Rev. Lett. **111**, 170405 (2013).  
 [15] O. Hul, O. Tymoshchuk, S. Bauch, P. M. Koch, and L. Sirko, J. Phys. A: Math. Gen. **38**, 10489 (2005).  
 [16] M. Lawniczak, O. Hul, Szymon Bauch, Petr Seba, Leszek Sirko Phys. Rev. E **77**, 056210 (2008).  
 [17] U. Kuhl, H.-J. Stöckmann, and R. Weaver, J. Phys. A: Math. Gen. **38**, 10433 (2005).  
 [18] N. Søndergaard, T. Guhr, M. Oxborrow, K. Schaadt, and C. Ellegaard Phys. Rev. E **70**, 036206 (2004).  
 [19] A. Morales, J. Flores, L. Gutiérrez, and R. A. Méndez-Sánchez, J. Acoust. Soc. Am. **112**, 1961 (2002).  
 [20] A. Arreola-Lucas, J. A. Franco-Villafañe, G. Báez, and R. A. Méndez-Sánchez, J. of Sound and Vibration **342**, 168 (2015).  
 [21] O. Xeridat, C. Poli, O. Legrand, F. Mortessagne, and P. Sebbah, Phys. Rev. E **80**, 035201(R) (2009).  
 [22] S. Catheline, N. Bénéch, J. Brum, and C. Negreira, Phys. Rev. Lett. **100**, 064301 (2008).  
 [23] A. Morales, A. Díaz-de-Anda, J. Flores, L. Gutiérrez, R. A. Méndez-Sánchez, G. Monsivais, and P. Mora, EPL **99**, 54002 (2012).  
 [24] O. I. Lobkis, I. S. Rozhkov, and R. L. Weaver, Phys. Rev. Lett., **91**, 194101 (2003).  
 [25] G. Báez, M. Cobián-Suárez, A. M. Martínez-Argüello, M. Martínez-Mares, and R. A. Méndez-Sánchez, Acta Phys. Pol. A **124**, 1069 (2013).  
 [26] A. Morales, L. Gutiérrez, and J. Flores, Am. J. Phys. **69**, 517 (2001).  
 [27] S. Hemmady, X. Zheng, E. Ott, T. M. Antonsen, and S. M. Anlage, Phys. Rev. Lett. **94**, 014102 (2005).  
 [28] A. M. Martínez-Argüello, R. A. Méndez-Sánchez, and M. Martínez-Mares, Phys. Rev. E. **86**, 016207 (2012).  
 [29] G. López, P. A. Mello, and T. H. Seligman, Z. Phys. A **302**, 351 (1981).  
 [30] P. A. Mello, P. Pereyra, and T. H. Seligman, Ann. Phys. (NY) **161**, 254 (1985).